Human Reproduction, Vol.35, No.8, pp. 1781–1796, 2020
Advance Access Publication on July 26, 2020 doi:10.1093/humrep/deaa151

human reproduction

ORIGINAL ARTICLE *Early pregnancy*

Periconceptional exposure to lopinavir, but not darunavir, impairs decidualization: a potential mechanism leading to poor birth outcomes in HIV-positive pregnancies

Smriti Kala[1], Caroline Dunk[2], Sebastian Acosta[1], and Lena Serghides[1,3,*]

[1]Toronto General Hospital Research Institute, University Health Network, Toronto, ON, Canada [2]Lunenfeld-Tanenbaum Research Institute, Mount Sinai Hospital, Toronto, ON, Canada [3]Department of Immunology and Institute of Medical Sciences, University of Toronto, Toronto, ON, Canada

*Correspondence address. Toronto General Hospital Research Institute, University Health Network, Princess Margaret Cancer Research Tower, 101 College Street, 10th Floor, Suite 10-359, Toronto, ON M5G 1L7, Canada. E-mail lena.serghides@utoronto.ca

Submitted on April 3, 2020; resubmitted on May 18, 2020; editorial decision on May 29, 2020

STUDY QUESTION: Does HIV protease inhibitor (PI)-based combination antiretroviral therapy (cART) initiated at periconception affect key events in early pregnancy, i.e. decidualization and spiral artery remodeling?

SUMMARY ANSWER: Two PIs, lopinavir and darunavir, currently offered as cART options in HIV-positive pregnancies were evaluated, and we found that lopinavir-based cART, but not darunavir-based cART, impaired uterine decidualization and spiral artery remodeling in both human *ex vivo* and mouse *in vivo* experimental models.

WHAT IS KNOWN ALREADY: Early initiation of cART is recommended for pregnant women living with HIV. However, poor birth outcomes are frequently observed in HIV-positive pregnancies exposed to PI-based cART, especially when it is initiated prior to conception. The correlation between early initiation of PI-cART and adverse birth outcomes is poorly understood, due to lack of data on the specific effects of PI-cART on the early stages of pregnancy involving uterine decidualization and spiral artery remodeling.

STUDY DESIGN, SIZE, DURATION: Lopinavir and darunavir were evaluated in clinically relevant combinations using an *ex vivo* human first-trimester placenta-decidua explant model, an *in vitro* human primary decidual cell culture system, and an *in vivo* mouse pregnancy model. The first-trimester (gestational age, 6–8 weeks) human placenta-decidua tissue was obtained from 11 to 15 healthy women undergoing elective termination of pregnancy. C57Bl/6 female mice (four/treatment group) were administered either lopinavir-cART, darunavir-cART or water by oral gavage once daily starting on the day of plug detection until sacrifice.

PARTICIPANTS/MATERIALS, SETTING, METHODS: *Human*: Spiral artery remodeling was assessed by immunohistochemical analysis of first-trimester placenta-decidua explant co-culture system. Trophoblast migration was measured using a placental explant culture. A primary decidual cell culture was used to evaluate the viability of immune cell populations by flow cytometry. Soluble factors, including biomarkers of decidualization and angiogenesis, were quantified by ELISA and Luminex assay using decidua-conditioned media.
Mouse: In the mouse pregnancy model, gestational day 6.5 or 9.5 implantation sites were used to assess decidualization, spiral artery remodeling and uterine natural killer (uNK) cell numbers by immunohistochemistry. Transcription factor STAT3 was assayed by immunohistochemistry in both human decidua and mouse implantation sites.

MAIN RESULTS AND THE ROLE OF CHANCE: Lopinavir-cART, but not darunavir-cART, impaired uterine decidualization and spiral artery remodeling in both experimental models. Lopinavir-cART treatment was also associated with selective depletion of uNK cells, reduced trophoblast migration and defective placentation. The lopinavir-associated decidualization defects were attributed to a decrease in expression of transcription factor STAT3, known to regulate decidualization. Our results suggest that periconceptional initiation of

lopinavir-cART, but not darunavir-cART, causes defective maturation of the uterine endometrium, leading to impairments in spiral artery remodeling and placentation, thus contributing to the poor birth outcomes.

LARGE SCALE DATA: N/A

LIMITATIONS, REASONS FOR CAUTION: The human first-trimester placenta/decidua samples could only be obtained from healthy females undergoing elective termination of pregnancy. As biopsy is the only way to obtain first-trimester decidua from pregnant women living with HIV on PI-cART, ethics approval and participant consent are difficult to obtain. Furthermore, our animal model is limited to the study of cART and does not include HIV. HIV infection is also associated with immune dysregulation, inflammation, alterations in angiogenic factors and complement activation, all of which could influence decidual and placental vascular remodeling and modify any cART effects.

WIDER IMPLICATIONS OF THE FINDINGS: Our findings provide mechanistic insight with direct clinical implications, rationalizing why the highest adverse birth outcomes are reported in HIV-positive pregnancies exposed to lopinavir-cART from conception. We demonstrate that dysregulation of decidualization is the mechanism through which lopinavir-cART, but not darunavir-cART, use in early pregnancy leads to poor birth outcomes. Although lopinavir is no longer a first-line regimen in pregnancy, it remains an alternate regimen and is often the only PI available in low resource settings. Our results highlight the need for reconsidering current guidelines recommending lopinavir use in pregnancy and indicate that lopinavir should be avoided especially in the first trimester, whereas darunavir is safe to use and should be the preferred PI in pregnancy.

Further, in current times of the COVID-19 pandemic, lopinavir is among the top drug candidates which are being repurposed for inclusion in clinical trials world-over, to assess their therapeutic potential against the dangerous respiratory disease. Current trials are also testing the efficacy of lopinavir given prophylactically to protect health care workers and people with potential exposures. Given the current extraordinary numbers, these might include women with early pregnancies, who may or may not be cognizant of their gestational status. This is a matter of concern as it could mean that women with early pregnancies might be exposed to this drug, which can cause decidualization defects. Our findings provide evidence of safety concerns surrounding lopinavir use in pregnancy, that women of reproductive age considering participation in such trials should be made aware of, so they can make a fully informed decision.

STUDY FUNDING/COMPETING INTEREST(S): This work was supported by funding from the Canadian Institutes of Health Research (CIHR) (PJT-148684 and MOP-130398 to L.S.). C.D. received support from CIHR Foundation (FDN143262 to Stephen Lye). S.K. received a TGHRI postdoctoral fellowship. The authors declare that there are no conflicts of interest. L.S. reports personal fees from ViiV Healthcare for participation in a Women and Transgender Think Tank.

Key words: HIV protease inhibitors / lopinavir / darunavir / decidualization / spiral artery remodeling / trophoblasts / uterine natural killer cells / birth outcomes / drug safety / COVID-19

Introduction

Combination antiretroviral therapy (cART) is now recommended for all pregnant women living with HIV, for maternal health and to prevent vertical HIV transmission (Money *et al.*, 2014; Lundgren *et al.*, 2015; WHO Guidelines, 2015). Current guidelines recommend early initiation of cART; therefore, the number of pregnancies exposed to cART at periconception is constantly rising. However, many studies associate the use of cART in pregnancy with higher rates of adverse outcomes, including miscarriage, preterm birth (PTB), low birth weight (LBW) and small for gestational age (SGA) birth (Chen *et al.*, 2012; Fowler *et al.*, 2016; Li *et al.*, 2016; Mofenson, 2016; Saleska *et al.*, 2018). Adverse outcomes seem more frequent with protease inhibitor-based cART regimens (PI-cART) and with initiation of therapy prior to conception (Kourtis *et al.*, 2007; Chen *et al.*, 2012; Sibiude *et al.*, 2012; Li *et al.*, 2016; Van Dyke *et al.*, 2016; Zash et al., 2017; Snijdewind *et al.*, 2018; Wang *et al.*, 2018). A knowledge gap exists regarding the specific effects of PI-cART exposure on early gestational events including decidualization, implantation and placentation, which occur during periconception.

Decidualization is a dramatic morphological and functional transformation of the uterine endometrium to form the decidua—the maternal face of the placenta, in species with hemochorial (invasive) placentation. In contrast to most of these species, decidualization of human endometrium does not require embryo implantatio but occurs in every menstrual cycle in response to stimulation by the ovarian hormones, progesterone and estrogen (Bhurke *et al.*, 2016; Vinketova *et al.*, 2016). During decidualization, endometrial stromal cells (ESCs) differentiate into specialized secretory decidual stromal cells (DSCs). If fertilization occurs, the process of decidualization continues facilitated by DSC-secreted hormonal factors that allow for blastocyst implantation (Gellersen and Brosens, 2014). Following successful implantation, decidual spiral arteries begin remodeling into highly dilated vessels to supply adequate maternal blood to the placenta and meet the increasing metabolic demands of the fetus (Whitley and Cartwright, 2010). In the early or 'trophoblast independent' stage, spiral artery remodeling is driven by uterine natural killer (uNK) cells, which account for ~70% of all maternal leukocytes infiltrating the decidua (Smith *et al.*, 2009; Hazan *et al.*, 2010; Lima *et al.*, 2014). uNK cells surround the spiral arteries and are a rich source of cytokines and angiogenic factors that may prime the spiral arteries for trophoblast invasion (Dunk *et al.*, 2008). In the advanced or 'trophoblast dependent' stage of spiral artery remodeling, extravillous trophoblasts (EVTs) migrate from trophoblast cell columns at the tips of the placental villi and invade the decidual spiral arteries (Kaufmann *et al.*, 2003). This results in degradation of endothelial and smooth muscle cells in spiral arteries and incorporation of EVTs within the vascular walls, thereby transforming the spiral arteries from narrow caliber, high resistance to large caliber, low

resistance vessels (Burton *et al.*, 2009). The successful completion of decidualization and subsequent remodeling of spiral arteries is crucial to optimal placentation and fetal development, and therefore to overall pregnancy outcome.

Based on data from a clinical cohort of PI-cART exposed pregnant women living with HIV, we previously showed that exposure to PI-cART during pregnancy was associated with lower levels of progesterone that correlated with lower birth weight (Papp *et al.*, 2015). This correlation was also observed in a mouse pregnancy model, where supplementation with progesterone partially reversed the PI-cART induced fetal growth restriction (Papp *et al.*, 2015). We also reported higher estradiol levels in maternal and cord plasma of PI-cART exposed pregnant women living with HIV, and found that cord estradiol levels were inversely correlated with birth weight centile (Balogun *et al.*, 2018). The optimum balance between progesterone and estrogen is crucial for creating a suitable endometrial environment for implantation, and for uterine and placental angiogenesis. While PI-cART exposure alters placental vasculature (Mohammadi *et al.*, 2018), it remains unknown whether or not uterine remodeling is affected by the initiation of periconceptional PI-cART. This gap in knowledge needs to be addressed because current treatment guidelines advocate early initiation of cART, and growing evidence points to higher rates of adverse birth outcomes among women who initiated PI-cART before pregnancy or in first trimester (Kourtis *et al.*, 2007; Chen *et al.*, 2012; Sibiude *et al.*, 2012; Li *et al.*, 2016; Van Dyke *et al.*, 2016; Zash et al., 2017; Snijdewind *et al.*, 2018; Wang *et al.*, 2018).

Hence, the objective of this study was to investigate whether PI-cART initiated at periconception affects decidualization and spiral artery remodeling in early pregnancy. Two PIs, lopinavir and darunavir, currently offered as cART options in human HIV-positive (HIV+) pregnancies, were evaluated in clinically relevant combinations using an *ex vivo* first-trimester human placenta-decidua explant model, an *in vitro* primary decidual cell culture system, and an *in vivo* mouse pregnancy model. As uterine remodeling is dependent on regulated levels of progesterone and estrogen, we hypothesized that the dysregulation of hormones by PI-cART will impair optimal decidualization and spiral artery remodeling, contributing to inefficient placentation and therefore poor birth outcomes.

Materials and methods

Drug regimens

Lopinavir, darunavir, ritonavir (r), zidovudine and lamivudine were obtained from the National Institutes of Health AIDS Reagent Program, dissolved in dimethyl sulphoxide (DMSO) to make 12 000× stocks, aliquoted and stored at −20°C until use. Drugs were thawed at room temperature and diluted to 200× in culture medium (RPMI or DMEM) containing 1 mg/ml BSA to avoid precipitation, followed by further dilution to 1× in the culture medium. 1× equals the C_{max} concentration of the drug in human pregnancy (Kala *et al.*, 2018)—the concentrations have been listed in Supplementary Table SI. Tissues/cells were incubated with the following drug combinations: ritonavir-boosted lopinavir (lopinavir/r)-cART = [lopinavir + ritonavir + zidovudine + lamivudine] or ritonavir-boosted darunavir (darunavir/r)-cART= [darunavir + ritonavir + zidovudine + lamivudine]. The final concentration of DMSO in the culture medium was 0.025% (v/v).

Drugs administered to the mice were purchased as prescription drugs. Drug doses yielding human therapeutic plasma concentrations were used (Kala *et al.*, 2018). Animals were administered either lopinavir/r-cART= [lopinavir/r (133/33.3 mg/kg/day) with zidovudine + lamivudine (100 + 50 mg/kg/day)], darunavir/r-cART = [darunavir/r (40/5 mg/kg/day) with zidovudine + lamivudine (100 + 50 mg/kg/day)] or water as a control. Pulverized tablets were dissolved in sterile water and administered by oral gavage.

Tissue collection and preparation

Human.

First-trimester placentae and/or decidua parietalis samples were obtained from healthy women undergoing elective terminations of pregnancy between 6 and 9 weeks of gestation. Fresh tissue was collected in ice-cold PBS and processed within 2 h of collection.

Mouse.

Housing conditions, breeding and drug treatment of mice have been described previously (Papp *et al.*, 2015). Eight to 10 weeks old, plugged C57Bl/6 females were randomly assigned into a treatment arm, and administered either lopinavir/r-cART, darunavir/r-cART or water by oral gavage once daily starting on the day of plug detection (gestational day (GD) 0.5) until sacrifice. On GD 6.5, pregnant dams (n = 4/treatment group) were sacrificed by CO_2 inhalation. The uterine horn was dissected and the number of implantation sites counted. Individual implantation sites were collected and immersed in 4% (v/v) paraformaldehyde for 1 h at room temperature for fixation, and then stored in 70% (v/v) ethanol at 4°C until processing. On GD 9.5, pregnant dams (n = 4/treatment group) were sacrificed by cervical dislocation. Euthanasia by CO_2 asphyxiation was avoided to prevent vasodilation of uterine arteries. Prior to uteri removal, dental floss was tied around the cervix and the distal end of each uterine horn, proximal to the ovaries, to ligate the uterine artery and prevent arterial collapse (Kieckbusch *et al.*, 2015). Intact uteri were excised distally to the three ligation points and the number of implantation sites counted. To preserve the original size and shape of utero-placental vasculature, whole uteri were stretched along the same long-axis and secured to a polystyrene block, then immersed in 10% (v/v) formalin overnight at 4°C. Excess uterine adipose tissue was trimmed and individual implantation sites were collected from the uterine membrane, then stored in 70% (v/v) ethanol at 4°C until processing into paraffin using a Shandon Excelsior ES (Thermo Scientific) automated tissue processor. Processed implantation sites were carefully sliced in the plane perpendicular to the long-axis of the uterus, and embedded in paraffin, cut side facing down. Serial sections of 5 µm thickness were cut at the midsagittal point and stained with hematoxylin-eosin (H&E) to evaluate morphology.

First-trimester human placenta-decidua explant co-culture

Placenta-decidua co-culture was performed as described previously (Dunk *et al.*, 2003). Briefly, fresh tissues were collected and assessed for quality. Small sections of decidua parietalis with a solid structure and intact luminal epithelium were dissected. Intact villi with EVT

columns were carefully dissected from the matched placenta (same donor). Decidua pieces were incubated in serum-free media (DMEM-F12, phenol red free, Gibco) containing drugs or DMSO (0.025% (v/v) final concentration) for 2 h at 37°C. These were then placed at a 45 degree angle, epithelial side facing up, on cell culture inserts (0.4 μm, 12 mm diameter, EMD Millipore) pre-coated with 120 μl matrigel (undiluted, high concentration, phenol red-free, Corning), and placed in a 24-well plate. The matrigel was allowed to solidify, followed by careful placement of placental villous explants on the decidual epithelial surface. Four hundred microliters of serum-free DMEM-F12 medium supplemented with normocin, progesterone (20 ng/ml) and estradiol (0.3 ng/ml) (N+P4+E2) was placed outside the insert and tissues were incubated overnight at 37°C with 3% O_2, 5% CO_2 and balanced N_2. Next morning, the placental explants were further anchored with 30 μl of matrigel. Tissues were then covered with 200 μl of supplemented (N+P4+E2) serum-free DMEM-F12 medium containing drugs or DMSO and allowed to incubate for an additional 5 days, during which the media inside and outside the insert was changed once. The tissues were fixed in 4% (v/v) paraformaldehyde for 1 h, washed with PBS, dehydrated in ascending concentrations of ethanol, cleared in xylene and embedded in paraffin. Blocks were sectioned to 5 μm thickness and every 10th serial section was histologically assessed by standard H&E staining. Explants from each donor were cultured in triplicate for each treatment group. The experiment was repeated with placenta-decidua matched tissues from five different donors. Decidua-alone samples served as a control to ensure that there was no trophoblast invasion prior to setting up the co-culture.

To quantify the depth of remodeling, co-culture sections immunostained for CK-7, SMA and CD31 were imaged and signs of progressive remodeling were tracked along the depth of the decidua as previously described (Hazan *et al.*, 2010). Measurements were made from the epithelial surface up to the midsegment of the decidua (0–1000 μm) showing advanced or early stages of vascular transformation. CK-7 positive *en*EVTs were scored as present (within the vessel lumen) or absent. Five independent experiments from five different donors, each with two to three explants per treatment group, were quantified.

First-trimester human placental villous explant culture

EVT-containing villi were dissected from placenta tissue, positioned on cell culture inserts pre-coated with 200 μl matrigel, and placed in a 24-well plate. Four hundred microliters of serum-free media (DMEM-F12, phenol red free) supplemented with normocin was placed outside the insert and the explants were incubated overnight at 37°C with 3% O_2 and 5% CO_2. Next morning, all successfully attached explants were randomly assigned to a treatment group. The villous explants were either treated with media containing drugs (or DMSO) in the absence or presence of decidua-conditioned medium (DCM). The DCM was a pool of (filtered) culture supernatants obtained from several individual primary decidual cell cultures, treated with either lopinavir/r-cART, or darunavir/r-cART, or DMSO. The explants were photographed after 48 h of drug treatment, using a Leica DFC400 camera attached to a dissecting microscope. ImageJ software (NIH, USA) was used to measure the area of EVT outgrowth. Seven independent experiments, each with three to four villous explants per treatment group, were quantified by a reviewer blinded to treatment allocation.

First-trimester human decidual cell culture

Decidual tissue was processed as described previously, with modifications (Wright *et al.*, 2006). Tissue was thoroughly washed in PBS to remove blood clots and finely minced with scalpels in a small volume of RPMI 1640 medium (serum and phenol red free) containing 50 μg/ml gentamicin. Tissue fragments were digested in a cocktail of 1 mg/ml collagenase (type IV, Worthington), 0.1 mg/ml trypsin inhibitor, 0.15 mg/ml DNaseI and 1 mg/ml BSA for 45 min at 37°C. At the end of the incubation, cells were chilled on ice and the enzymes were inactivated with 10% (v/v) fetal bovine serum (FBS). Decidual cells were collected via filtration through a 70 μm cell strainer and centrifugation at 500*g* for 10 min at 4°C. The supernatant was discarded, the cell pellet was washed once with serum-free medium and finally resuspended in serum-free RPMI 1640 medium (phenol red free) supplemented with 1× MEM non-essential amino acids (Gibco), 1× glutamax (Gibco), 10 mM HEPES, 1 mM sodium pyruvate and 50 μg/ml gentamycin. Cells were plated on a 24-well plate at a density of 1×10^6 cells/well, in the presence of progesterone (100 nM), estradiol (10 nM) and cAMP (20 μM). Cells were exposed to DMSO (control) or drugs at C_{max} concentration (as described above) for 48 h at 37°C in a 5% CO_2 incubator; following which, the cells were harvested and used for flow cytometric analysis and aliquots of the culture supernatant were stored at −20°C until tested by ELISA or multiplex assays. Alamar Blue (Life Technologies) was used as per the manufacturer's instructions to determine cellular viability to control for differences in the number of live cells. Experiments were performed in triplicate and repeated 13–15 times.

Flow cytometry

One million cells from each treatment group of the human decidual cell culture were washed with PBS and incubated for 30 min on ice with Live Dead dye (fixable viability dye eFluor780, Invitrogen) followed by a wash in stain buffer (with FBS, BD Pharmingen). Cells were incubated with 10% (v/v) human serum for 15 min on ice to block non-specific antibody binding sites, followed by incubation with fluorochrome-conjugated mouse monoclonal antibodies for 30 min on ice. Cells were washed in stain buffer and fixed in 2% (v/v) paraformaldehyde for 30 min on ice, followed by an additional wash. Cells were then analyzed using a BD LSRII flow cytometer and data analysis was performed using FlowJo V10. Cell debris and aggregates were excluded by gating on forward versus side scatter, then by height versus area of forward scatter plots prior to population discrimination. Live cells were gated using a viability dye that marks all dead cells. The gates for leukocyte sub-populations were set within CD45-expressing cells as follows: uNK cells (CD45 and CD56 positive, CD16 negative), macrophages (CD45 and CD14 positive) and T cells (CD45 and CD3 positive). The gate for DSCs was set within CD45 negative cells, positive for CD90. Fluorescence minus one controls were used to set appropriate gates during analysis. Antibodies used are listed in Supplementary Table SII.

Luminex assay

Reagents for Luminex® assay were custom developed by R&D Systems. Human decidual cell culture supernatants (n = 15) were screened to measure 17 analytes which were divided into two panels.

Panel 1 included the following nine analytes: Endoglin, VEGF, MMP-8, prolactin, IGFBP-1, CXCL16, GM-CSF, IL-15 and PlGF. Panel 2 included the following eight analytes: MMP-9, CXCL12, CXCL10, CCL2, angiopoietin-2, IFN-γ, CCL3 and IL-11. Undiluted culture supernatants were used to perform the assay according to the manufacturer's instructions. Standards and samples were run in duplicates and serum-free medium was assayed as blank control. Plates were read immediately on the MAGPIX instrument and raw data were analyzed using the xPONENT software. The % CV between the duplicates was <5%. Values outside the lower limit of quantification were assigned a value of one-third of the lower limit of the standard curve. The concentration of each analyte per decidual sample was calculated in picogram per milliliter and corrected for the number of live cells per treatment group. The standard range of all the analytes is reported in Supplementary Table SIII.

ELISA

Activin-A was measured in undiluted decidual culture supernatants (n = 11) using the human activin-A duoset ELISA kit (R&D Systems) as per the manufacturer's protocol. The concentrations were calculated in picogram per milliliter and corrected for the number of live cells per treatment group. Total STAT3 was measured in decidual cell lysates (n = 8) using the human STAT3 ELISA kit (Abcam ab176666) as per the manufacturer's protocol. Cell lysates were prepared from 2×10^6 cells per treatment group and were in the range of 100–500 µg/ml of total protein. Lysates were aliquoted and stored at −80°C and assayed within a month. Total STAT3 concentrations were calculated in microgram per milliliter, corrected for total protein concentration per treatment group, and normalized to the control, which was set at 100%.

Immunohistochemical analysis

Immunohistochemical analysis was performed on 5 µm sections using the streptavidin peroxidase method as described previously (Hazan *et al.*, 2010). Antigen retrieval was performed by microwaving the slides in 10 mM sodium citrate (pH 6) or 1 mM EDTA (pH 9). Slides were blocked using serum-free protein blocking solution (Dako) for 1 h at room temperature, followed by overnight incubation at 4°C in primary antibody (Supplementary Table SII). Subsequent incubations with anti-mouse (1:300, Dako) or anti-rabbit (1:1000, Abcam) biotinylated secondary antibody and streptavidin-horseradish peroxidase-conjugated tertiary reagent (Invitrogen) were carried out for 1 h each at room temperature. Incubation with mouse IgG (Dako) or rabbit IgG (Abcam) in place of primary antibody served as a negative control. Specific signals were detected using a Liquid DAB+ (3,3-diaminobenzidine) Chromogen System (Dako). Slides were counterstained using Gill's No.1 hematoxylin (Sigma-Aldrich), dehydrated in ascending series of ethanol, cleared in xylene and mounted with Cytoseal (Thermo Fisher Scientific). Photographs were taken with an Olympus DP72 camera mounted on a BX61 Olympus microscope using the CellSens Standard program or the slides were scanned at 20× magnification with Aperio AT2 brightfield scanner.

The images were quantified by either the newCAST software (Visiopharm) or by digital imaging analysis software; HALO (Indica Labs). Quantification of CD56 positive uNK cells and pSTAT3 staining in human decidua samples was performed by Visiopharm. The region of interest was identified using a masking tool and the total area was recorded in two replicates for the same biological sample. Counts were performed using a standard protocol that assigned random counting frames covering 5% of each total masked tissue area. Brown cells (positively staining) and blue cells (negatively staining) were counted at 10× magnification. A positively stained ratio was generated by dividing the total numbers of positively staining cells by the total number of cells counted in the tissue area.

Quantification of mouse immunostained tissues was performed by using the Cytonuclear IHC module of HALO software. The region of interest was identified in each image and the settings were set to include the full range of staining intensity (weak to strong). Cells stained with an intensity exceeding the settings threshold were counted as positive. Data were collected as the number of positive cells divided by the tissue area scanned.

Immunofluorescence

Sections were dewaxed and rehydrated followed by antigen retrieval. Autofluorescence was blocked using 1% (w/v) Sudan black in 70% (v/v) ethanol for 1 min. Non-immune block (10% (v/v) goat serum) was applied for 1 h at room temperature followed by overnight incubation with pan-keratin mouse monoclonal antibody at 4°C (Supplementary Table SII). Goat anti-mouse Alexa Fluor-488 conjugated secondary antibody (Invitrogen) was applied at 1:200 dilution, together with DAPI nuclear counterstain for 1 h at room temperature. Sections were mounted using Shandon Immu-Mount (Fisher Scientific). Negative control included omission of primary antibody to control for autofluorescence. Slides were stored at 4°C in dark until scanned.

Statistical analysis

Graphing and statistical analyses were conducted using GraphPad Prism 7.0 (GraphPad Software Inc.). Normality of all data was assessed using the Shapiro–Wilk normality test, and all data were normally distributed. Comparisons of multiple groups were evaluated using one-way ANOVA, without matching or pairing followed by Tukey's post-test. For multiplex data analysis of secreted decidual proteins, differences between multiple groups were evaluated using repeated measures one-way ANOVA with Tukey's post-test. Results were deemed statistically significant when $P < 0.05$.

Study approval

This study was carried out in accordance with the recommendations of Mount Sinai Hospital Research Ethics Board, Sinai Health System. The protocol was approved by the Mount Sinai Hospital Research Ethics Board, Sinai Health System REB# 02-0061A and University Health Network Research Ethics Board REB# 15-9661. All subjects gave written informed consent in accordance with the Declaration of Helsinki. Informed consent was obtained through the BioBank program at the Research Centre for Women's and Infants' Health at Mount Sinai Hospital using the above mentioned REB approved protocol. All research using human tissues was performed in a class II certified laboratory by qualified staff trained in biological and chemical safety protocols, and in accordance with Health Canada guidelines and regulations.

Animal experiments were approved by the University Health Network Animal Use Committee (REB approval number 2575.25)

and performed according to the policies and guidelines of the Canadian Council on Animal Care.

Results

Lopinavir treatment impairs spiral artery remodeling in a human placenta-decidua explant co-culture system

To investigate the effect of PIs on decidual spiral artery remodeling, we employed a human placenta-decidua explant co-culture system previously shown to emulate uterine vascular adaptations during the first trimester (Dunk *et al.*, 2003) (Fig. 1). Placental-decidual co-cultures were treated with either lopinavir boosted with ritonavir (lopinavir/r) (abbreviated as LPV/r in figures), or darunavir boosted with ritonavir (darunavir/r) (abbreviated as DRV/r in figures), or DMSO (final concentration 0.025% (v/v)) as a control. Tissue sections were stained with cytokeratin-7 (CK-7) to assess trophoblast invasion, CD31 or smooth muscle actin (SMA) to assess presence or loss of endothelial cells and smooth muscle cells, respectively, around vessels, or CD45 to assess leukocyte location around vessels.

In both the darunavir/r and control co-cultures, trophoblast invasion of spiral arteries could be observed. CK-7$^+$ endovascular EVTs (*en*EVTs) could be seen invading the lumen of arteries traversing the region of decidua in close proximity to the placenta (see arrows in Fig. 1A and I). The invaded arteries in both the control and darunavir/r co-cultures displayed advanced stages of remodeling, evident by a complete loss of endothelial (lack of CD31 staining) (see arrows in Fig. 1B and J) and smooth muscle cells (lack of SMA staining) (see arrows in Fig. 1C and K) lining the vessel walls. The expected leukocyte recruitment to the site of vascular remodeling could also be seen (Fig. 1D and L).

In contrast, in the lopinavir/r treated co-cultures vessel remodeling was impaired. Although EVTs were released from the placenta, *en*EVT invasion of spiral arteries was not seen, as evident from absence of CK-7 staining inside the vessel lumen (see arrows in Fig. 1E). Robust CD31 (see arrows in Fig. 1F) and SMA staining (see arrows in Fig. 1G) were seen around the vessel walls, indicating un-remodeled vessels with intact endothelial and smooth muscle cells. Although leukocytes were present, their accumulation around the vessels was impaired in the lopinavir/r treated co-cultures (see arrows in Fig. 1H).

A decidua-alone culture (in the absence of placental explants) was used to rule out any sign of spiral artery remodeling before the setup of co-culture (Fig. 1M–P). The control decidua was negative for CK-7, and non-invaded vessels stained positive for SMA and CD31.

Similar results were obtained from five independent co-culture experiments, each using matched placenta-decidua tissue from different donors. Summed data from all the co-culture experiments indicate that in the proximal part of the decidua, close to the site of placental-decidual contact, 80% of the arteries in the control group and 73% in the darunavir/r group were fully remodeled and showed trophoblast invasion. In contrast, none of the arteries in the lopinavir/r group were fully remodeled, and only 26% of the arteries showed signs of the early stages of vascular transformation, i.e. partial loss of smooth muscle cells and endothelium, and absence of trophoblast invasion. On the basis of these criteria, the depth of remodeling from the decidual epithelial surface up to the midsegment of the decidua was calculated and found to be significantly lower in the lopinavir/r group, compared to control and darunavir/r (Fig. 1Q).

Lopinavir treatment inhibits trophoblast migration in a human placental explant culture

Since EVTs play an important role in decidual vascular remodeling, especially in the advanced stages of remodeling, the effects of PI-cART on EVT outgrowth were investigated using human villous explants with EVT cell columns dissected from first-trimester placentas. No pronounced differences in EVT outgrowth were observed between treatment groups when villi were treated with lopinavir/r, lopinavir/r-cART, darunavir/r-cART or DMSO (Supplementary Fig. S1).

EVT migration relies in part on chemo-attractant signals provided by the decidua. We repeated the EVT migration experiments in the presence of DCM obtained from primary decidual cell cultures treated with the same drugs (or DMSO). While a healthy EVT outgrowth was seen upon exposure to DCM from DMSO or darunavir/r-cART-treated cultures, EVT outgrowth was impeded upon exposure to DCM from lopinavir/r-cART or lopinavir/r alone treated cultures (Fig. 2).

In summary, EVT migration was impaired in the presence of lopinavir/r-DCM. EVT outgrowth was unaffected by drug treatment in the absence of DCM, suggesting that lopinavir's impact on EVT migration is likely due to effects on decidua-secreted factors rather than direct effects on EVTs.

Lopinavir treatment leads to depletion of uNK cells in a primary culture of human decidual cells

Decidua immune cells, comprised of uNK cells, T cells, dendritic cells and macrophages, also play an important role in the early stages of decidual vascular remodeling. We next investigated the effects of PI-cART on total decidual cell cultures. Total cells were isolated from human first-trimester decidua samples and cultured in the presence of drugs, or DMSO as a control, for 48 h followed by flow cytometric analysis. The gating strategy is shown (Supplementary Fig. S2). The percentage of total viable cells was reduced upon lopinavir/r and lopinavir/r-cART treatment, but was similar to the control upon darunavir/r-cART treatment, indicating that lopinavir was associated with loss of cellular viability (Fig. 3A). Further analysis of decidual subpopulations revealed that the viability of stroma cells, macrophages and T cells did not differ between treatments. However, the viability of uNK cells was significantly lower in the lopinavir/r and lopinavir/r-cART groups, as compared to control and darunavir/r-cART (Fig. 3A). Thus, exposure of primary decidual cell cultures to lopinavir resulted in selective depletion of uNK cells. Macrophages are also known to influence vascular remodeling, but no significant differences were observed in CD14+ macrophage populations across treatments. Macrophage subset analysis was not performed, but may be merited for future studies.

To confirm the flow cytometry data, we also stained placental-decidual co-cultures with CD56 to detect uNK cells (Fig. 3B). Fewer uNK cells were detected in co-cultures treated with lopinavir/r

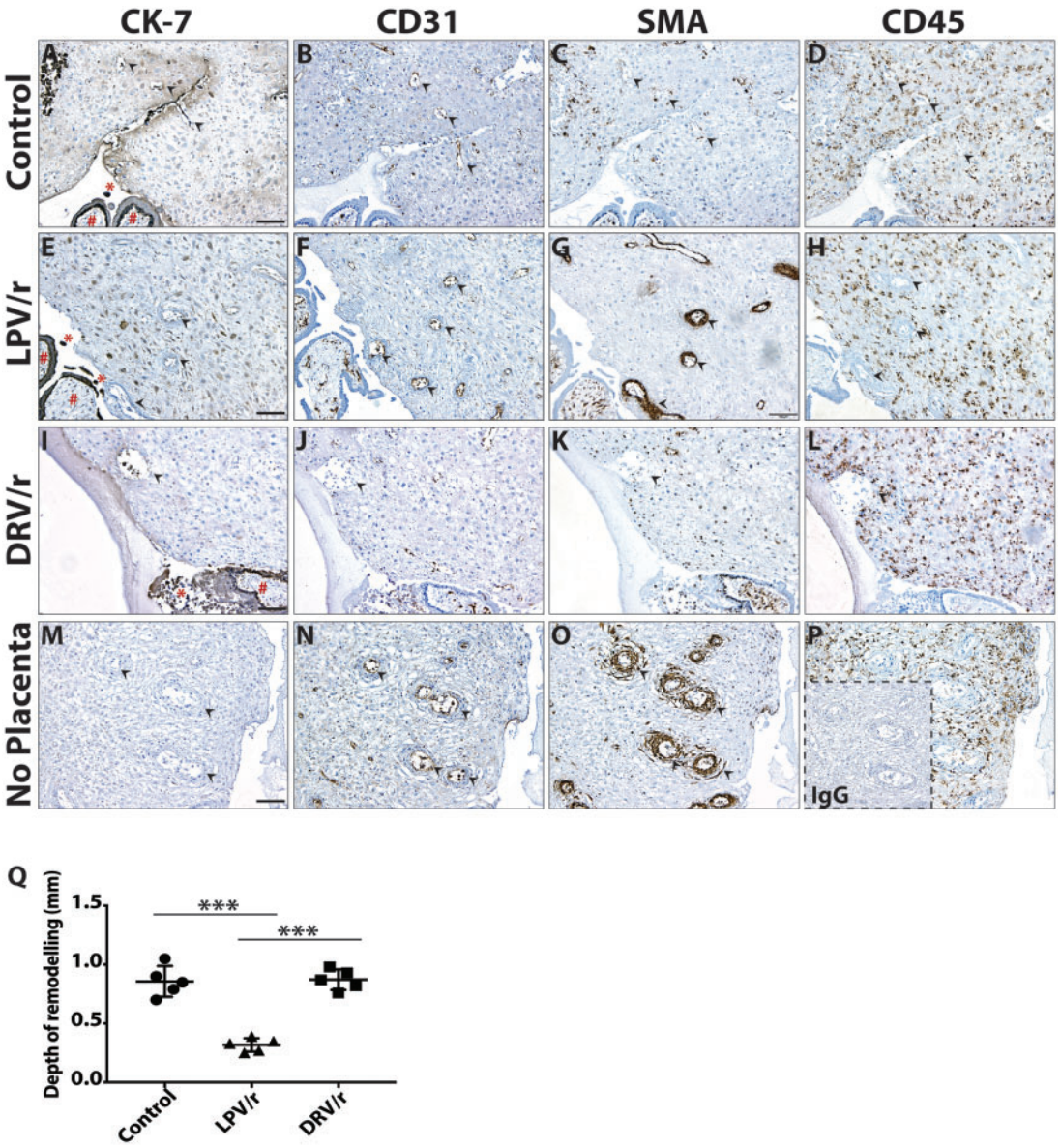

Figure 1. Lopinavir treatment impairs spiral artery remodeling in a human placenta-decidua explant co-culture system. Immunohistochemical assessment of remodeling vessels in serial cross-sections of placental-decidual co-cultures, treated with protease inhibitors (PIs) or DMSO control as indicated. Representative images of immunostaining with cytokeratin-7 (CK-7; marker for trophoblasts), CD31 and smooth muscle actin (SMA) (markers for spiral arteries), and CD45 (marker for leukocytes) are shown. (**A–D**) Complete vascular transformation in co-cultures treated with DMSO (control) and (**I–L**) ritonavir-boosted darunavir (DRV/r) as indicated. (**A, I**) Placenta tissue (#) is in close contact with the decidua, and CK-7 positive extravillous trophoblasts (EVTs; *) were released from the placenta. Endovascular EVTs (*En*EVTs) were present within the lumen of spiral arteries (arrows). (**B, J**) The invaded arteries displayed loss of CD31 positive endothelial cells and (**C, K**) complete removal of SMA positive cells lining the vessel walls. (**D, L**) CD45 staining showed leukocyte enrichment at the site of vascular remodeling. (**E–H**) Impairment of vascular remodeling in co-culture treated with ritonavir-boosted lopinavir (LPV/r). (**E**) The placenta (#) is in close contact with the decidua and CK-7 positive EVTs (*) were released, but there was a complete lack of *En*EVT invasion of spiral arteries (arrows). (**F**) Non-invaded arteries retained CD31 positive endothelium and (**G**) intact rings of SMA. (**H**) CD45 positive leukocytes were evenly distributed, but sparsely surrounded the vessels. (**M–P**) Decidua parietalis cultured in the absence of placenta. (**M**) The tissue was negative for CK-7. (**N**) Non-invaded arteries stained robustly for CD31 and (**O**) SMA. (**P**) CD45 positive leukocytes were spread evenly throughout the tissue. Inset is negative control: non-immune mouse IgG. Scale bars, 100 μm. (**Q**) Quantification of the depth of remodeling in co-cultures. Results are the mean ± SD. *** indicates $P < 0.0001$, calculated using ANOVA with Tukey's *post hoc* analysis. Each data point represents the average of two to three measurements per experiment; n = 5 independent experiments.

compared to control or darunavir/r treated co-cultures (Fig. 3C). In addition, uNK cells in the lopinavir/r treated co-cultures showed a condensed appearance, characteristic of apoptotic cells (see arrows in Fig. 3B, middle panel).

Lopinavir treatment of human decidual cell cultures results in a decline in the levels of biomarkers of decidualization, chemokines and angiogenic factors

Our data so far suggested that lopinavir/r treatment impacts both decidual immune cell composition, i.e. uNK cells, and decidual soluble factors that affect EVT migration. To further examine the impact of PI-cART on decidua function, we quantified soluble factors in DCM. Primary human decidual cells (total) were cultured in the presence of progesterone, estradiol and cAMP to maintain the decidual phenotype *in vitro* and treated with drugs or DMSO as a control.

Levels of the classic biomarkers of decidualization, including prolactin, IGFBP-1, IL-11, IL-15 and activin-A were significantly lower in the supernatants of decidual cell cultures treated with lopinavir/r or lopinavir/r-cART compared to control (Table I), suggesting that lopinavir exposure leads to a loss of the decidual phenotype. Levels of these factors in cultures treated with darunavir/r-cART were similar to control.

Levels of CXCL10, CXCL12, CXCL16, CCL2 and CCL3 chemokines that play a role in immune cell recruitment and trophoblast chemotaxis were also significantly lower in decidual cell cultures treated with lopinavir/r or lopinavir/r-cART, but were similar to control in cultures treated with darunavir/r-cART (Table I).

Levels of the angiogenic factors VEGF, PlGF, angiopoietin-2, GM-CSF, IFN-γ and MMP-9 were significantly lower with lopinavir/r or lopinavir/r-cART, but not with darunavir/r-cART treatment, compared to control (Table I). Levels of endoglin and MMP-8 were similar in all treatment groups.

Collectively these data show that lopinavir treatment of human decidual cells results in a reduction in secretion of factors involved in decidualization, chemotaxis and angiogenesis, suggesting altered decidua cell function and a loss of the decidual phenotype with lopinavir exposure.

Lopinavir treatment is associated with impaired decidualization and spiral artery remodeling, and lower uNK cells in a mouse pregnancy model

We next sought to confirm our findings of impairments in decidualization, decidual function and spiral artery remodeling in the context of lopinavir/r treatment in an *in vivo* system using a murine model.

Decidualization.

To test the effect of PI-cART on the process of decidualization, we collected GD 6.5 implantation sites from mice treated once daily orally with PI-cART (yielding plasma drug levels approximating human minimal effective concentrations), or water as a control. GD6.5 implantation sites were slightly smaller (not significant) in the lopinavir/r-cART group as compared to darunavir/r-cART and control groups. H&E staining indicated that implantation site morphology was similar, with successful embryo implantation observed in all the treatment groups, although uterine lumen closure seemed to be delayed in the lopinavir/r-cART group (Supplementary Fig. S3).

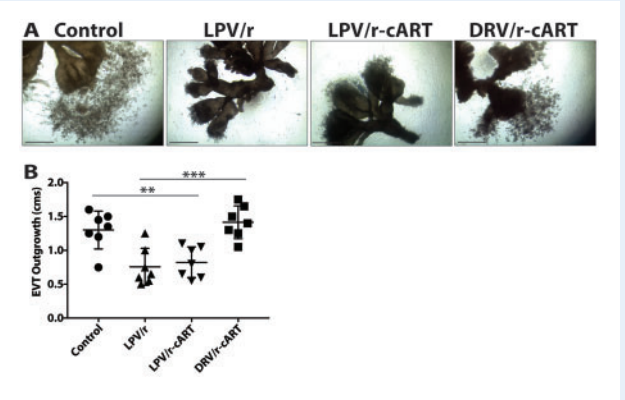

Figure 2. Lopinavir treatment inhibits trophoblast migration in a human placental explant culture. (**A**) Explants from first-trimester placentas treated with DMSO (control) or protease inhibitors (PIs) as indicated, and cultured in the presence of decidua-conditioned medium (DCM) obtained from primary decidual cell culture also treated with the same drugs (or DMSO). Representative images are shown. Scale bars, 1 cm. (**B**) Extravillous trophoblast (EVT) outgrowth was measured at the termination of the experiment (66 h). Results are the mean ± SD. *** indicates $P < 0.0001$, calculated using ANOVA with Tukey's *post hoc* analysis. Each data point represents the average of three replicates per experiment; n = 7 independent experiments. cART, combination antiretroviral therapy; DRV/r, ritonavir-boosted darunavir; LPV/r, ritonavir-boosted lopinavir.

To evaluate the extent of decidualization, GD6.5 implantation sites were immunostained with anti-Ki67 antibody, a marker for cellular proliferation (Fig. 4A). A robust decidual response was observed in the implantation sites of control and darunavir/r-cART-treated mice, marked by intense Ki67 staining in the secondary decidual zone (SDZ) and the mesometrial decidua, indicative of extensive stromal cell proliferation (Fig. 4A and B). In lopinavir/r-cART-treated mice, Ki67+ cells in the mesometrial decidua were dramatically reduced, while only weakly Ki67+ cells were observed in the SDZ (Fig. 4A and B). Ki67 staining was not observed in the primary decidual zone (PDZ) across all treatments. These data show that lopinavir treatment is associated with less proliferation in the stromal compartments, indicative of impaired decidualization.

Spiral artery remodeling.

To investigate the effect of PI-cART on spiral artery remodeling, we collected GD9.5 implantation sites (Fig. 4C, upper panels). Number of implantation sites (9 ± 1) did not differ between treatment groups at this gestational stage; however, implantation sites were slightly smaller (not significant) and more frequently displayed signs of resorption (dark spots) in the lopinavir/r-cART group. To quantify degree of spiral artery remodeling, spiral artery lumen area in the decidua basalis was assessed by stereology (Fig. 4C, lower panels). Mean vessel lumen area was significantly lower in the lopinavir/r-cART group compared to control or darunavir/r-cART, indicative of reduced spiral artery

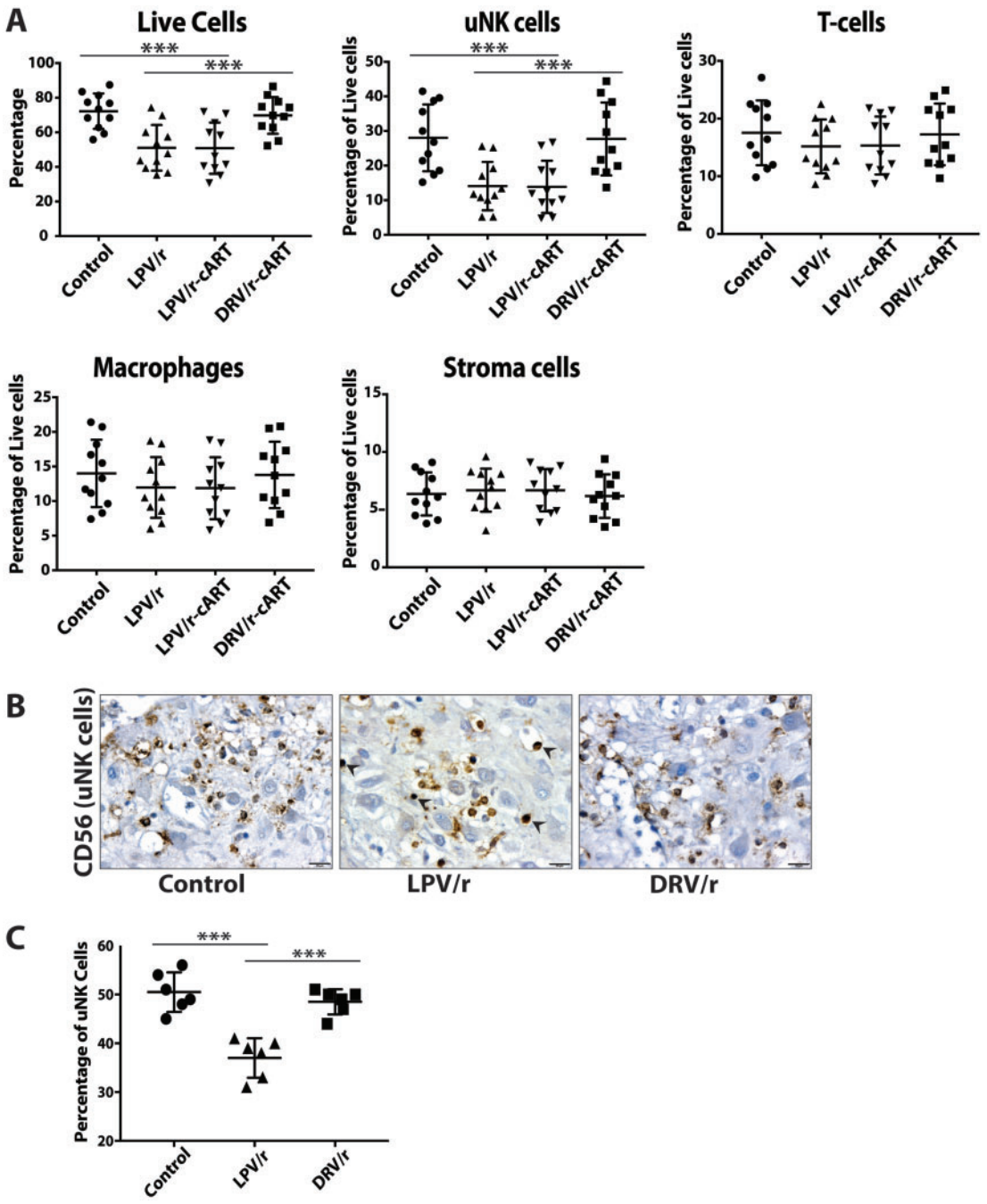

Figure 3. Lopinavir treatment leads to depletion of uterine NK cells in a primary culture of human decidual cells. (**A**) Quantification of flow cytometry data showing total live cells and leukocyte subsets from the primary human decidual cell cultures treated with DMSO (control) or protease inhibitors (PIs) as indicated. Results are the mean ± SD. *** indicates *P*-value < 0.0001, calculated using ANOVA with Tukey's *post hoc* analysis. For T cells, macrophages and stroma cells, *P*-value was not significant between the treatment groups. Each data point represents the average of two replicates per experiment; n = 11 independent experiments. (**B**) Representative images of CD56 immunostaining of uterine NK (uNK) cells in first-trimester decidua treated with DMSO (control) or PIs as indicated. In the ritonavir-boosted lopinavir (LPV/r) treatment group, uNK cells display a condensed appearance (arrows), characteristic of apoptotic cells. Scale bar, 20 μm. (**C**) Stereological quantification of CD56 positive uNK cells. Results are the mean ± SD. *** indicates $P < 0.0001$, calculated using ANOVA with Tukey's *post hoc* analysis. Each data point represents the average of two to three replicates per experiment; n = 6 independent experiments. cART, combination antiretroviral therapy; DRV/r, ritonavir-boosted darunavir.

Table I Multiplex analysis of secreted proteins of human decidual cell culture treated with ritonavir-boosted lopinavir (lopinavir/r), lopinavir/r-combined antiretroviral therapy (cART), ritonavir-boosted darunavir (darunavir/r)-cART, or DMSO (control) as indicated.

		Mean (SEM), pg/ml			
		Control (*N* = 15)	Lopinavir/r (*N* = 15)	Lopinavir/r-cART (*N* = 15)	Darunavir/r-cART (*N* = 15)
Biomarkers of decidualization	Prolactin	623 (30)	341 (20)[a,b]	342 (21)[a,b]	627 (32)
	IGFBP-1	32 802 (1625)	25 553 (1795)[a,b]	24 813 (1637)[a,b]	31 414 (1824)
	IL-15	7.1 (0.44)	5.1 (0.46)[a,b]	4.9 (0.47)[a,b]	7.3 (0.48)
	IL-11	835 (135)	507 (77)[a,b]	529 (84)[a,b]	784 (131)
	Activin-A	542 (34)	225 (3)[a,b]	214 (21)[a,b]	507 (35)
Chemokines	CXCL10	216 (49)	106 (23)[a,b]	108 (25)[a,b]	195 (47)
	CXCL12	300 (34)	237 (28)[a,b]	230 (28)[a,b]	290 (33)
	CXCL16	97 (16)	26 (4.1)[a,b]	25 (3.7)[a,b]	94 (16)
	CCL2	2281 (684)	1301 (458)[a,b]	1351 (481)[a,b]	2094 (610)
	CCL3	4649 (659)	3412 (489)[a,b]	3374 (486)[a,b]	4222 (577)
Pro-angiogenic factors	VEGF	25 (3.3)	16 (2.2)[a,b]	17 (2.0)[a,b]	24 (3.5)
	PlGF	18.8 (2.1)	12.4 (1.4)[a,b]	12.9 (1.3)[a,b]	19.3 (2.2)
	Ang2	198 (29)	112 (19)[a,b]	106 (18)[a,b]	199 (30)
	GM-CSF	88 (22)	48 (10)[a,b]	50 (11)[a,b]	86 (20)
	IFN-γ	58 (9)	38 (6)[a,b]	39 (7)[a,b]	59 (11)
	MMP-9	13 046 (1766)	4820 (713)[a,b]	4493 (712)[a,b]	11 696 (1432)
	MMP-8	495 (34)	485 (33)	492 (35)	528 (36)
	Endoglin	503 (24)	493 (25)	502 (38)	520 (28)

All protein concentrations are in pg/ml. Results are presented as mean with standard error of the mean (SEM). Differences between groups were evaluated using repeated measures one-way ANOVA with Tukey's post-test.
[a]$P < 0.05$ versus control.
[b]$P < 0.05$ versus darunavir/r-cART.
n = 15 independent experiments.

remodeling (Fig. 4D). Consistent with the findings of smaller vessel lumen areas in the lopinavir/r-cART group, SMA staining demonstrated the presence of entire rings of smooth muscle cells around spiral arteries (Fig. 4E and F), indicative of un-remodeled vessels. In contrast, intensity of SMA staining was significantly reduced, with only specks of SMA remaining in spiral arteries of control and darunavir/r-cART groups (Fig. 4E and F), suggestive of a successful remodeling process.

uNK cell.

To assess the impact of PI-cART on the early contributions of uNK cells to decidual remodeling, GD9.5 implantation sites were stained with DBA-lectin, a marker for murine uNK cells. As expected in midgestation, uNK cells were abundant in the decidua basalis of both control and darunavir/r-cART-treated mice (Fig. 5A–C), with uNK cells surrounding the spiral arteries and frequently invading their lumen (Fig. 5A, lower panels). In contrast, the number of uNK cells was significantly reduced in the decidua basalis of lopinavir/r-cART-treated mice (Fig. 5A–C) and vascular infiltration by the uNK cells was reduced (see arrows in Fig. 5A, lower panels). The apoptotic-cell like condensed appearance seen in the uNK cells in the human co-cultures was also noticeable in the mouse (indicated by * in Fig. 5A, lower panel).

Lopinavir treatment is associated with defective placentation and developmental retardation in a mouse pregnancy model

Given the observed impact of lopinavir on the decidua, we explored whether this would influence placenta and fetal development. By midgestation, the structure of the early placenta begins to form, and the three distinct placental layers namely, the labyrinthine trophoblast, spongiotrophoblast and giant cell layers, can be readily identified. Immunostaining of implantation sites with the pan trophoblast cell marker cytokeratin revealed that placental morphology differed in the lopinavir/r-cART treated mice compared to the other groups (Fig. 6). In the placentae of control and darunavir/r-cART-treated mice, trophoblasts migrated centrally into the decidua and only one or two layers of parietal trophoblast giant cells (P-TGCs) were visible. In contrast, the placentae of lopinavir/r-cART-treated mice did not exhibit a centrally directed invasive front and displayed an increased number of P-TGC layers (Fig. 6, middle panel). Prospective spongiotrophoblast and labyrinth layers were diminished, and fewer fetal blood vessels were seen in the developing labyrinth of lopinavir/r-cART compared to control or darunavir/r-cART-treated mice (Supplementary Fig. S4). It was also noted that in a minority of lopinavir/r-cART-treated mice, chorioallantoic fusion had failed to occur. Additionally, H&E-stained midsagittal sections of the GD9.5 implantation sites revealed an abnormal

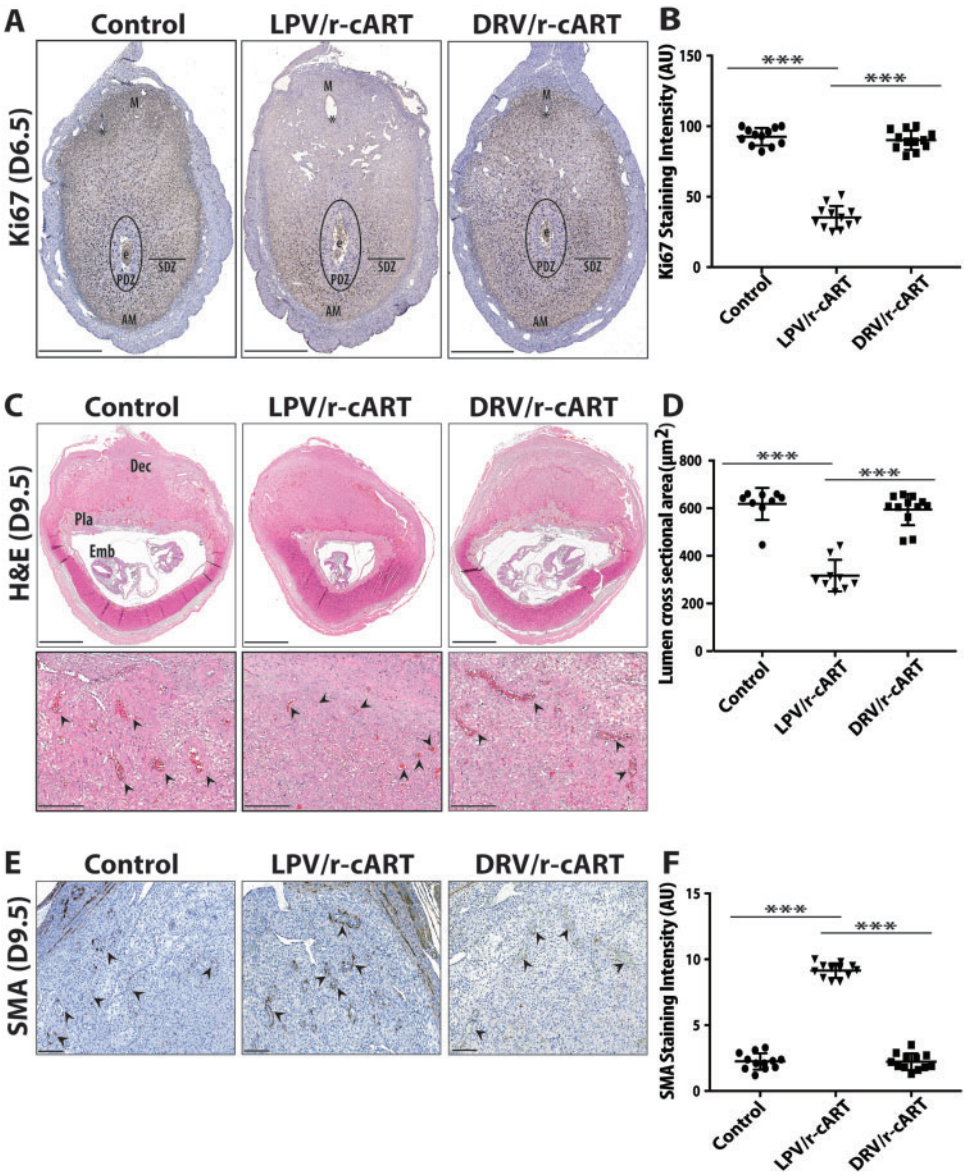

Figure 4. Lopinavir treatment causes decidualization defects and impairs spiral artery remodeling in a mouse pregnancy model. (**A**) Representative images of Ki67 immunostaining of proliferative cells in midsaggital sections from GD 6.5 implantation sites of control, ritonavir-boosted lopinavir (LPV/r)-combination antiretroviral therapy (cART) and ritonavir-boosted darunavir (DRV/r)-cART-treated mice. E, embryo; PDZ, primary decidual zone; SDZ, secondary decidual zone; M, mesometrium; AM, anti-mesometrium. * indicates uterine lumen. Scale bar, 600 μm. (**B**) Quantification of staining intensity (pixels) of Ki67 positive cells. Results are the mean ± SD. *** indicates $P < 0.0001$, calculated using ANOVA with Tukey's *post hoc* analysis. Each data point represents an implantation site, three implantation sites were analyzed per mouse (n = 4 mice/treatment group). (**C**) Representative images of H&E-stained midsaggital sections from GD9.5 implantation sites of control, LPV/r-cART and DRV/r-cART-treated mice. Dec, decidua; Emb, embryo; Pla, placenta. Lower panels show a magnified view of the decidua basalis to highlight the spiral arteries (indicated by arrows). Scale bar, 1 mm (upper panels), 200 μm (lower panels). (**D**) Quantification of lumen areas of spiral arteries. Results are the mean ± SD. *** indicates $P < 0.0001$, calculated using ANOVA with Tukey's *post hoc* analysis. Each data point represents an implantation site, and is the average of 15 measurements (5 measurements per section, 3 sections per implantation site); 2–3 implantation sites were analyzed per mouse (n = 4 mice/treatment group). (**E**) Representative images of smooth muscle actin (SMA) immunostaining of the spiral arteries (indicated by arrows) in decidua basalis region of GD9.5 implantation sites of control, LPV/r-cART and DRV/r-cART-treated mice. Scale bar, 200 μm. (**F**) Quantification of staining intensity (pixels) of SMA positive cells. Results are the mean ± SD. *** indicates $P < 0.0001$, calculated using ANOVA with Tukey's *post hoc* analysis. Each data point represents an implantation site, three implantation sites were analyzed per mouse (n = 4 mice/treatment group).

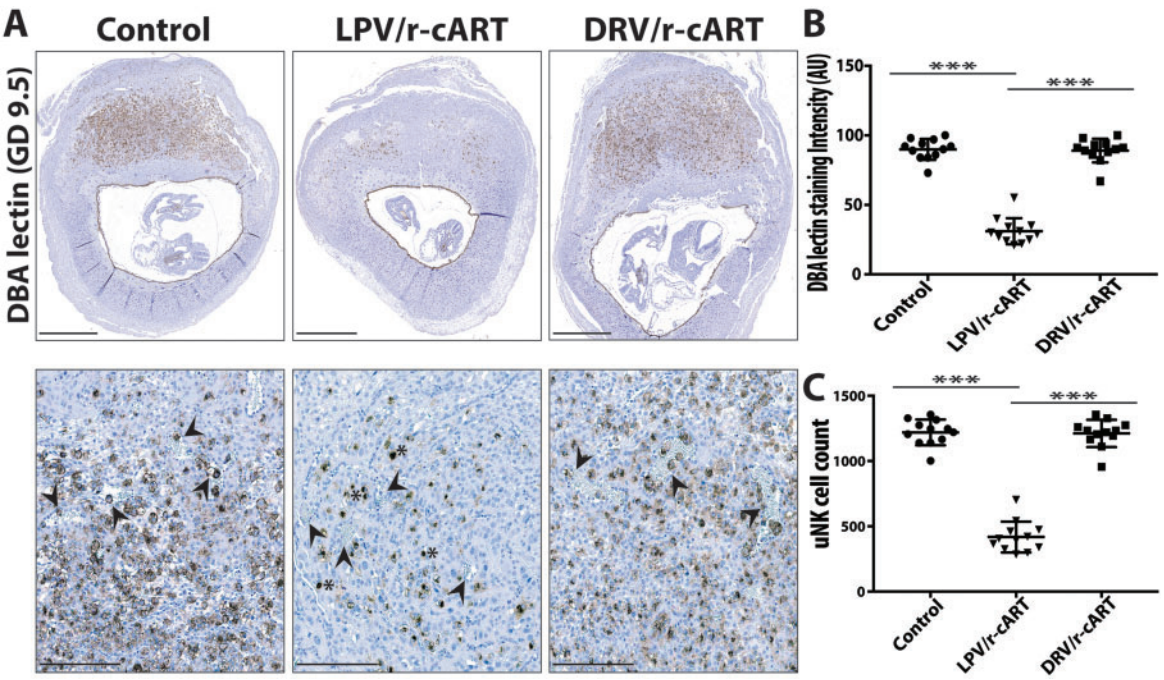

Figure 5. Lopinavir treatment leads to depletion of uterine NK cells in a mouse pregnancy model. (**A**) Representative images of DBA-lectin immunostaining of the uterine NK (uNK) cells in decidua basalis region of GD9.5 implantation sites of control, ritonavir-boosted lopinavir (LPV/r)-combination antiretroviral therapy (cART) and ritonavir-boosted darunavir (DRV/r)-cART-treated mice. Lower panels show a magnified view of the decidua basalis to highlight the uNK cell infiltration of the spiral arteries (indicated by arrows). The condensed apoptotic appearance of uNK cells in the LPV/r-cART treatment is indicated by *. Scale bar, 1 mm (upper panels), 200 μm (lower panels). (**B**) Quantification of staining intensity (pixels) of DBA-lectin positive uNK cells and **(C)** uNK cell counts for each treatment group. Results are the mean ± SD. *** indicates $P < 0.0001$, calculated using ANOVA with Tukey's *post hoc* analysis. Each data point represents an implantation site, three implantation sites were analyzed per mouse (n = 4 mice/treatment group).

progression of fetal development in the lopinavir/r-cART group, likely indicating developmental retardation (Fig. 4C, upper panels).

Lopinavir treatment inhibits the transcription factor STAT3

Our data, thus far, strongly support that lopinavir exposure in early pregnancy has a negative impact on decidualization and spiral artery remodeling both in a human first-trimester decidua-placenta explant model and in a murine model. We next explored the mechanisms that could underlie these effects. Progesterone-dependent decidualization of uterine endometrium is mediated by cyclic AMP (cAMP), which induces the expression or activation of the core decidual transcription factors, including signal transducer and activator of transcription (STAT)-3 (Gellersen and Brosens, 2014). In decidual stroma cells, STAT3 is activated by phosphorylation and phosphorylated STAT3 (pSTAT3) is transported from the cytoplasm into the nucleus, where it activates the expression of target genes such as *prolactin* and *igfbp-1*, the classic biomarkers of decidualization (Vinketova *et al.*, 2016). Silencing of STAT3 in human ESCs retards decidualization (Jiang *et al.*, 2015), emphasizing the critical role of STAT3 signaling in this process (Zhang *et al.*, 2015). We hypothesized that lopinavir may influence decidualization by impairing STAT3 signaling.

Lysates from first-trimester human decidual cell cultures treated with lopinavir/r or lopinavir/r-cART showed lower levels of total STAT3 protein as compared to lysates from cultures treated with darunavir/r-cART or DMSO (Supplementary Fig. S5). As the transcriptional function of STAT3 is activated upon its phosphorylation, we examined the effect of drug treatment on the level of pSTAT3 in decidual tissue of both human and mouse. First-trimester human decidua tissue treated with lopinavir/r-cART showed weaker pSTAT3 immunostaining in the nuclei of stromal cells as compared to decidua samples treated with darunavir/r-cART or DMSO (Fig. 7A and B). Consistent with these observations, mouse GD6.5 implantation sites stained with pSTAT3, also revealed significantly lower levels of pSTAT3 in the lopinavir/r-cART treatment group as compared to darunavir/r-cART and control (Fig. 7C and D). The pattern of pSTAT3 staining was similar to that of Ki67 staining, indicating an overlap between proliferating and decidualizing stromal compartments. The lopinavir/r-cART-treated mice displayed a significant reduction in the number of cells stained positively for pSTAT3 in the mesometrial decidua and SDZ of the implantation sites (Fig. 7C and D). Our data suggest that lopinavir treatment may cause decidual defects by interfering

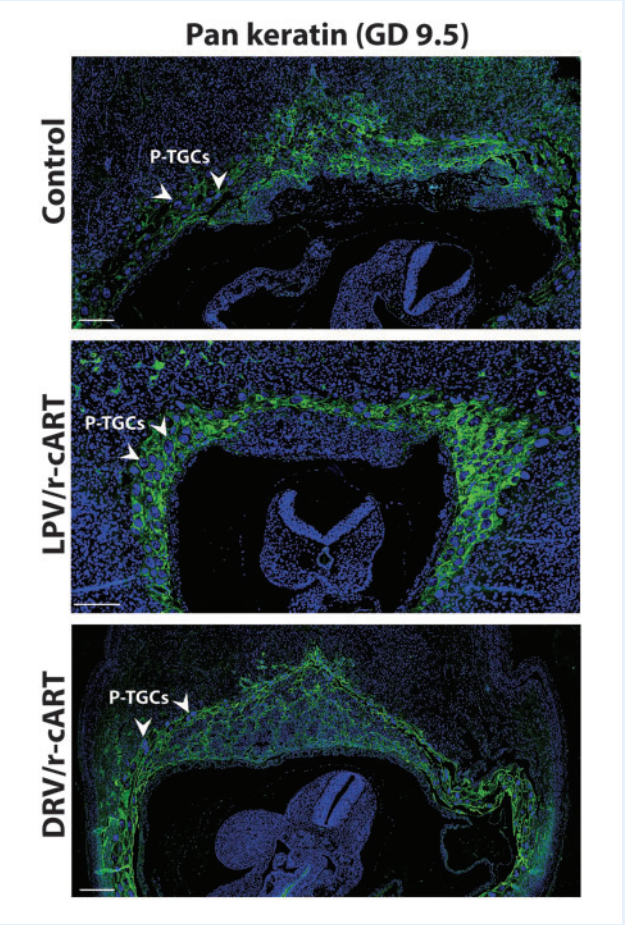

Figure 6. Lopinavir treatment causes defective placentation in a mouse pregnancy model. Representative images of pan-cytokeratin immunostaining (green) of trophoblasts in the placentas of GD 9.5 implantation sites of control, ritonavir-boosted lopinavir (LPV/r)-combination antiretroviral therapy (cART) and ritonavir-boosted darunavir (DRV/r)-cART-treated mice. DAPI, used for nuclear staining is blue. Parietal trophoblast giant cells (P-TGCs) with large, polyploid nuclei are indicated. Scale bar, 200 μm.

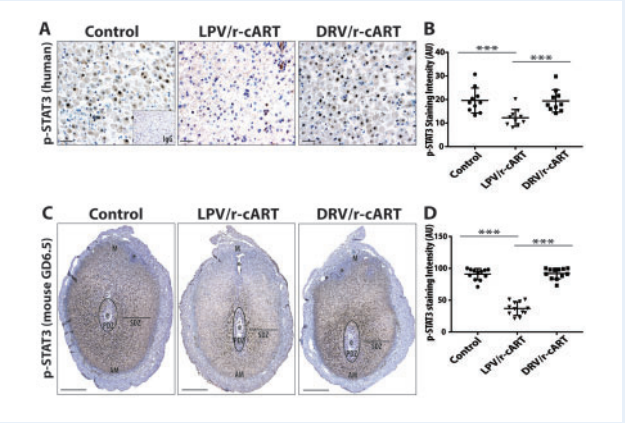

Figure 7. Lopinavir treatment inhibits the transcription factor STAT3. (**A**) Representative images of phosphorylated signal transducer and activator of transcription 3 (p-STAT3) immunostaining of stroma cells in first-trimester human decidua treated with DMSO (control) or protease inhibitor (PI)-combination antiretroviral therapy (cART) as indicated. Inset is negative control. Scale bar, 50 μm. (**B**) Quantification of staining intensity (pixels) of p-STAT3 positive stroma cells. Results are the mean ± SD. *** indicates $P < 0.0001$, calculated using ANOVA with Tukey's *post hoc* analysis. Each data point represents the average of two to three replicates per experiment; n = 10 independent experiments. (**C**) Representative images of p-STAT3 immunostaining of GD 6.5 implantation sites of control, ritonavir-boosted lopinavir (LPV/r)-cART and ritonavir-boosted darunavir (DRV/r)-cART treated mice. E, embryo; PDZ, primary decidual zone; SDZ, secondary decidual zone; M, mesometrium; AM, anti-mesometrium. * indicates uterine lumen. Scale bar, 600 μm. (**D**) Quantification of staining intensity (pixels) of p-STAT3 positive cells. Results are the mean ± SD. *** indicates $P < 0.0001$, calculated using ANOVA with Tukey's *post hoc* analysis. Each data point represents an implantation site, three implantation sites were analyzed per mouse (n = 4 mice/treatment group).

with STAT3 signaling which regulates stromal proliferation and differentiation.

Discussion

Periconception and first-trimester use of lopinavir-based cART has been linked to a higher incidence of adverse birth outcomes (Kourtis *et al.*, 2007; Chen *et al.*, 2012; Sibiude *et al.*, 2012; Li *et al.*, 2016; Van Dyke *et al.*, 2016; Zash et al., 2017; Snijdewind *et al.*, 2018; Wang *et al.*, 2018). We investigated the effects of PI-cART on uterine remodeling during early pregnancy using established models of first-trimester human placenta-decidua co-culture and mouse pregnancy. Here we present data, which demonstrate that initiation of lopinavir/r-based, but not darunavir/r-based cART from conception causes insufficient or defective maturation of the decidua during early pregnancy, leading to inadequate placentation that likely contribute to poor birth outcomes.

Our data from both human tissue and mouse studies are mutually supportive, and demonstrate that use of lopinavir/r-cART, but not darunavir/r-cART, impaired spiral artery remodeling and uterine decidualization. We observed the presence of un-remodeled vessels marked by intact SMA and endothelium, and a lack of EVT invasion in human placenta-decidua co-cultures treated with lopinavir/r. In the mouse model, we found that the lopinavir/r-cART group displayed spiral arteries with significantly smaller lumens and intact rings of SMA at GD9.5, indicative of impaired remodeling. Lopinavir treatment caused dysregulation of decidualization, as the secreted levels of the classic biomarkers of decidualization, prolactin, IGFBP-1, IL-11, IL-15 and activin-A, were significantly lower in the supernatants of primary decidual cell cultures treated with lopinavir/r-cART. Data from the mouse model further confirmed the defect in decidualization, as indicated by loss of proliferative Ki67+ cells in the stromal compartments of GD6.5 implantation sites of mice treated with lopinavir/r-cART. Lopinavir/r-cART was also associated with lower decidual levels of total and phosphorylated STAT3, a transcription factor known to

regulate decidualization. This could possibly explain the association between lopinavir/r exposure and failure to maintain the decidual phenotype.

During decidualization, differentiating stromal cells stimulated by progesterone produce a variety of chemokines and cytokines that trigger the recruitment of uNK cells and support their proliferation and survival in the decidua (Keskin *et al.*, 2007; Carlino *et al.*, 2008). In turn, uNK cells play a role in maintaining the decidual reaction in the stromal cells (Croy *et al.*, 2002). We found that the decidualization defects induced by lopinavir treatment were concomitant with lower levels of secreted chemokines (CXCL10, CXCL12, CXCL16, CCL2 and CCL3) in the primary decidual cell cultures, indicative of dysfunctional stromal cells. Lopinavir treatment was also associated with lower levels of IL-15, a key cytokine required for uNK proliferation and survival. Thus, the lower number of uNK cells and their frequent apoptotic-like phenotype observed in both decidual cultures and in mice treated with lopinavir/r-cART could be the result of defective decidua stromal cell function that led to both poor chemo-attraction of NK cells to the decidua, and poor support of their proliferation and survival.

uNK cells secrete various growth and angiogenic factors which are not only beneficial to decidua stromal cells but also play critical roles in remodeling of the decidual spiral arteries (Robson *et al.*, 2012). We found lower expression of a number of factors predominantly produced by uNK cells, such as VEGF, PlGF, angiopoietin-2, GM-CSF, IFN-γ and MMP-9, which aligns with the selective depletion of uNK cells upon lopinavir exposure of primary decidual cell cultures.

Our data suggested that lopinavir did not directly impair trophoblast migration, since EVT outgrowth in matrigel was not affected by drug treatment alone. However, trophoblast migration was reduced in response to lopinavir-treated DCM (obtained from primary decidual cell culture treated with lopinavir/r or lopinavir/r-cART), suggesting that lopinavir treatment indirectly affects trophoblast migration and invasion by disrupting decidual secretion of factors which play a key role in this process (Wright *et al.*, 2010).

The deficiencies in uterine decidualization, vessel remodeling and local immune cell number/profile were accompanied by malformations in early placental development at GD9.5 of mouse pregnancy. Lopinavir/r-cART treatment led to an overabundance of P-TGCs at the cost of spongiotrophoblast and labyrinth layers. This particular phenotype has been previously reported in mice with deletions in transcription factors such as Mash2 (Guillemot *et al.*, 1995; Tanaka *et al.*, 1997) and FOXA2 (Kelleher *et al.*, 2017). In the case of FOXA2, the phenotype was reported to be associated with defects in stroma cell decidualization, similar to our observation.

Some studies have reported that HIV infection and/or cART are associated with morphological changes in placentas such as hypervascularity and maternal vascular malperfusion (Kalk *et al.*, 2017; Obimbo *et al.*, 2019). We previously reported the effect of lopinavir/r-cART treatment on placenta development and fetal outcomes in mouse pregnancy. We showed that pregnant mice exposed to lopinavir/r-cART treatment at the onset of pregnancy had significantly lower levels of plasma progesterone, which was associated with lower fetal and placental weights (Papp *et al.*, 2015), as well as alterations in the placental vasculature at GD14.5 (Mohammadi *et al.*, 2018) and GD17.5 (Cahill *et al.*, 2019). Delaying the initiation of lopinavir/r-cART, or supplementing lopinavir/r-cART-treated mice with progesterone throughout pregnancy, prevented the associated placenta vascular changes and significantly improved fetal weights (Mohammadi *et al.*, 2018). We have now demonstrated that lopinavir/r-cART compromises the process of uterine remodeling during early pregnancy, leading to downstream effects on placenta formation or function that are either negative or fail to fully compensate for these early defects, thus are associated with poor outcomes.

Our study has some limitations. The human first-trimester placenta/decidua samples could only be obtained from healthy females undergoing elective termination of pregnancy. As biopsy is the only way to obtain first-trimester decidua from pregnant women living with HIV on PI-cART, ethics approval and participant consent are difficult to obtain. Furthermore, our animal model is limited to the study of cART and does not include HIV. HIV infection is also associated with immune dysregulation, inflammation, alterations in angiogenic factors and complement activation, all of which could influence decidual and placental vascular remodeling and modify any cART effects. The strength of our study is that we are able to pinpoint that among PIs, lopinavir but not darunavir-based cART leads to deficiencies in uterine decidualization and spiral artery remodeling. By using the same backbone (zidovudine plus lamivudine) with both PIs across all experiments, we are also able to rule out the association of zidovudine and lamivudine with early pregnancy defects. Our findings correlate well with the higher incidence of poor birth outcomes in pregnant women living with HIV who initiate lopinavir-based cART before conception or in the first trimester of pregnancy.

In conclusion, our results suggest that initiation of lopinavir/r-cART during periconception dysregulates decidualization, leading to reduced uNK cell numbers. These decidual defects hinder trophoblast invasion, spiral artery remodeling, placentation and consequently could lead to adverse birth outcomes in pregnancies exposed to lopinavir/r-cART from conception. Unlike lopinavir, darunavir/r-cART was not associated with any defects in the decidualization process. Although lopinavir is no longer a first-line regimen in pregnancy, it remains an alternate regimen in many guidelines. In low resource settings, lopinavir is often the only PI available in cases where first-line regimens fail. Current guidelines also recommend that if an HIV+ pregnancy is conceived on lopinavir/r-cART, the same therapy should be continued. Our data indicate that lopinavir-based cART should be avoided in the first trimester of pregnancy to improve endometrial maturation and facilitate normal placentation, which could possibly reduce the risk of poor birth outcomes. Alternate PIs, such as darunavir, should be preferred over lopinavir for use in pregnancy.

Furthermore, in current times of the COVID-19 pandemic, lopinavir/r is among the top drug candidates which are being repurposed for inclusion in clinical trials world-over (https://doi.org/10.1186/ISRCTN83971151), to assess their therapeutic potential against the dangerous respiratory disease. The efficacy of lopinavir/r given prophylactically to protect health care workers and people with potential exposures is also being tested (NCT04321174). Given the current extraordinary numbers, these might include women with early pregnancies, who may or may not be cognizant of their gestational status. This is a matter of concern as it could mean that women with early pregnancies might be exposed to this drug, which can cause decidualization defects. Our findings provide evidence of safety concerns surrounding lopinavir/r use in pregnancy that women of reproductive age

considering participation in such trials should be made aware of, so they can make a fully informed decision.

Supplementary data

Supplementary data are available at *Human Reproduction* online.

Acknowledgments

We thank the donors, RCWIH BioBank (CIHR MGC-13299), the Lunenfeld-Tanenbaum Research Institute and the UHN/Mount Sinai Hospital, Department of Obstetrics and Gynecology for the human specimens used in this study. We thank Dr B. Anne Croy for helpful discussions on the manuscript. We thank the Stephen Lye lab for access and support. We thank J. Zhang and M. Guzman Lenis for scientific support.

Authors' roles

S.K., C.D. and L.S. conceived the research and designed the experiments. S.K. performed experiments and analyzed data with help from C.D. and L.S. S.A. performed the mouse experiments and analyzed spiral artery lumen area calculations. S.K. wrote the initial draft of the manuscript, C.D. and L.S. reviewed and edited the manuscript. All authors read and approved the final manuscript.

Funding

This work was supported by funding from the Canadian Institutes of Health Research (CIHR) (PJT-148684 and MOP-130398 to L.S.). C.D. received support from CIHR Foundation (FDN143262 to Stephen Lye). S.K. received a Toronto General Hospital Research Institute (TGHRI) postdoctoral fellowship. The funders were not involved in the study design, collection, analysis or interpretation of data, in the writing of the report or in the decision to submit the paper for publication.

Conflict of interest

The authors declare that there are no conflicts of interest. L.S. reports personal fees from ViiV Healthcare for participation in a Women and Transgender Think Tank.

References

Balogun KA, Guzman Lenis MS, Papp E, Loutfy M, Yudin MH, MacGillivray J, Walmsley SL, Silverman M, Serghides L. Elevated levels of estradiol in human immunodeficiency virus-infected pregnant women on protease inhibitor-based regimens. *Clin Infect Dis* 2018;**66**:420–427.

Bhurke AS, Bagchi IC, Bagchi MK. Progesterone-regulated endometrial factors controlling implantation. *Am J Reprod Immunol* 2016; **75**:237–245.

Burton GJ, Woods AW, Jauniaux E, Kingdom JC. Rheological and physiological consequences of conversion of the maternal spiral arteries for uteroplacental blood flow during human pregnancy. *Placenta* 2009;**30**:473–482.

Cahill LS, Zhou YQ, Hoggarth J, Yu LX, Rahman A, Stortz G, Whitehead CL, Baschat A, Kingdom JC, Macgowan CK *et al.* Placental vascular abnormalities in the mouse alter umbilical artery wave reflections. *Am J Physiol Heart Circ Physiol* 2019;**316**: H664–H672.

Carlino C, Stabile H, Morrone S, Bulla R, Soriani A, Agostinis C, Bossi F, Mocci C, Sarazani F, Tedesco F *et al.* Recruitment of circulating NK cells through decidual tissues: a possible mechanism controlling NK cell accumulation in the uterus during early pregnancy. *Blood* 2008;**111**:3108–3115.

Chen JY, Ribaudo HJ, Souda S, Parekh N, Ogwu A, Lockman S, Powis K, Dryden-Peterson S, Creek T, Jimbo W *et al.* Highly active antiretroviral therapy and adverse birth outcomes among HIV-infected women in Botswana. *J Infect Dis* 2012;**206**:1695–1705.

Croy BA, Chantakru S, Esadeg S, Ashkar AA, Wei Q. Decidual natural killer cells: key regulators of placental development (a review). *J Reprod Immunol* 2002;**57**:151–168.

Dunk C, Petkovic L, Baczyk D, Rossant J, Winterhager E, Lye S. A novel in vitro model of trophoblast-mediated decidual blood vessel remodeling. *Lab Invest* 2003;**83**:1821–1828.

Dunk C, Smith S, Hazan A, Whittle W, Jones RL. Promotion of angiogenesis by human endometrial lymphocytes. *Immunol Invest* 2008;**37**:583–610.

Fowler MG, Qin M, Fiscus SA, Currier JS, Flynn PM, Chipato T, McIntyre J, Gnanashanmugam D, Siberry GK, Coletti AS *et al.* Benefits and risks of antiretroviral therapy for perinatal HIV prevention. *N Engl J Med* 2016;**375**:1726–1737.

Gellersen B, Brosens JJ. Cyclic decidualization of the human endometrium in reproductive health and failure. *Endocr Rev* 2014;**35**: 851–905.

Guillemot F, Caspary T, Tilghman SM, Copeland NG, Gilbert DJ, Jenkins NA, Anderson DJ, Joyner AL, Rossant J, Nagy A. Genomic imprinting of Mash2, a mouse gene required for trophoblast development. *Nat Genet* 1995;**9**:235–242.

Hazan AD, Smith SD, Jones RL, Whittle W, Lye SJ, Dunk CE. Vascular-leukocyte interactions: mechanisms of human decidual spiral artery remodeling in vitro. *Am J Pathol* 2010;**177**:1017–1030.

Jiang Y, Liao Y, He H, Xin Q, Tu Z, Kong S, Cui T, Wang B, Quan S, Li B *et al.* FoxM1 directs STAT3 expression essential for human endometrial stromal decidualization. *Sci Rep* 2015;**5**:13735.

Kala S, Watson B, Zhang JG, Papp E, Guzman Lenis M, Dennehy M, Cameron DW, Harrigan PR, Serghides L. Improving the clinical relevance of a mouse pregnancy model of antiretroviral toxicity; a pharmacokinetic dosing-optimization study of current HIV antiretroviral regimens. *Antiviral Res* 2018;**159**:45–54.

Kalk E, Schubert P, Bettinger JA, Cotton MF, Esser M, Slogrove A, Wright CA. Placental pathology in HIV infection at term: a comparison with HIV-uninfected women. *Trop Med Int Health* 2017;**22**: 604–613.

Kaufmann P, Black S, Huppertz B. Endovascular trophoblast invasion: implications for the pathogenesis of intrauterine growth retardation and preeclampsia. *Biol Reprod* 2003;**69**:1–7.

Kelleher AM, Peng W, Pru JK, Pru CA, DeMayo FJ, Spencer TE. Forkhead box a2 (FOXA2) is essential for uterine function and fertility. *Proc Natl Acad Sci U S A* 2017;**114**:E1018–E1026.

Keskin DB, Allan DS, Rybalov B, Andzelm MM, Stern JN, Kopcow HD, Koopman LA, Strominger JL. TGFbeta promotes conversion of CD16+ peripheral blood NK cells into CD16- NK cells with similarities to decidual NK cells. *Proc Natl Acad Sci U S A* 2007; **104**:3378–3383.

Kieckbusch J, Gaynor LM, Colucci F. Assessment of maternal vascular remodeling during pregnancy in the mouse uterus. *J Vis Exp* 2015;**106**:e53534.

Kourtis AP, Schmid CH, Jamieson DJ, Lau J. Use of antiretroviral therapy in pregnant HIV-infected women and the risk of premature delivery: a meta-analysis. *AIDS* 2007;**21**:607–615.

Li N, Sando MM, Spiegelman D, Hertzmark E, Liu E, Sando D, Machumi L, Chalamilla G, Fawzi W. Antiretroviral therapy in relation to birth outcomes among HIV-infected women: a cohort study. *J Infect Dis* 2016;**213**:1057–1064.

Lima PD, Zhang J, Dunk C, Lye SJ, Croy BA. Leukocyte driven-decidual angiogenesis in early pregnancy. *Cell Mol Immunol* 2014; **11**:522–537.

Lundgren JD, Babiker AG, Gordin F, Emery S, Grund B, Sharma S, Avihingsanon A, Cooper DA, Fatkenheuer G, Llibre JM *et al*. Initiation of antiretroviral therapy in early asymptomatic HIV infection. *N Engl J Med* 2015;**373**:795–807.

Mofenson LM. Antiretroviral therapy and adverse pregnancy outcome: the elephant in the room? *J Infect Dis* 2016;**213**:1051–1054.

Mohammadi H, Papp E, Cahill L, Rennie M, Banko N, Pinnaduwage L, Lee J, Kibschull M, Dunk C, Sled JG *et al*. HIV antiretroviral exposure in pregnancy induces detrimental placenta vascular changes that are rescued by progesterone supplementation. *Sci Rep* 2018; **8**:6552.

Money D, Tulloch K, Boucoiran I, Caddy S. Guidelines for the care of pregnant women living with HIV and interventions to reduce perinatal transmission: executive summary. *J Obstet Gynaecol Can* 2014;**36**:721–734.

Obimbo MM, Zhou Y, McMaster MT, Cohen CR, Qureshi Z, Ong'ech J, Ogeng'o JA, Fisher SJ. Placental structure in preterm birth among HIV-positive versus HIV-negative women in Kenya. *J Acquir Immune Defic Syndr* 2019;**80**:94–102.

Papp E, Mohammadi H, Loutfy MR, Yudin MH, Murphy KE, Walmsley SL, Shah R, MacGillivray J, Silverman M, Serghides L. HIV protease inhibitor use during pregnancy is associated with decreased progesterone levels, suggesting a potential mechanism contributing to fetal growth restriction. *J Infect Dis* 2015;**211**:10–18.

Robson A, Harris LK, Innes BA, Lash GE, Aljunaidy MM, Aplin JD, Baker PN, Robson SC, Bulmer JN. Uterine natural killer cells initiate spiral artery remodeling in human pregnancy. *FASEB J* 2012;**26**: 4876–4885.

Saleska JL, Turner AN, Maierhofer C, Clark J, Kwiek JJ. Use of antiretroviral therapy during pregnancy and adverse birth outcomes among women living with HIV-1 in low- and middle-income countries: a systematic review. *J Acquir Immune Defic Syndr* 2018;**79**:1–9.

Sibiude J, Warszawski J, Tubiana R, Dollfus C, Faye A, Rouzioux C, Teglas JP, Ekoukou D, Blanche S, Mandelbrot L. Premature delivery in HIV-infected women starting protease inhibitor therapy during pregnancy: role of the ritonavir boost? *Clin Infect Dis* 2012;**54**: 1348–1360.

Smith SD, Dunk CE, Aplin JD, Harris LK, Jones RL. Evidence for immune cell involvement in decidual spiral arteriole remodeling in early human pregnancy. *Am J Pathol* 2009;**174**:1959–1971.

Snijdewind IJM, Smit C, Godfried MH, Bakker R, Nellen J, Jaddoe VWV, van Leeuwen E, Reiss P, Steegers EAP, van der Ende ME. Preconception use of cART by HIV-positive pregnant women increases the risk of infants being born small for gestational age. *PLoS One* 2018;**13**:e0191389.

Tanaka M, Gertsenstein M, Rossant J, Nagy A. Mash2 acts cell autonomously in mouse spongiotrophoblast development. *Dev Biol* 1997;**190**:55–65.

Van Dyke RB, Chadwick EG, Hazra R, Williams PL, Seage GR 3rd. The PHACS SMARTT Study: assessment of the safety of in utero exposure to antiretroviral drugs. *Front Immunol* 2016;**7**:199.

Vinketova K, Mourdjeva M, Oreshkova T. Human decidual stromal cells as a component of the implantation niche and a modulator of maternal immunity. *J Pregnancy* 2016;**2016**:8689436.

Wang L, Zhao H, Cai W, Tao J, Zhao Q, Sun L, Fan Q, Kourtis AP, Shepard C, Zhang F. Risk factors associated with preterm delivery and low delivery weight among HIV-exposed neonates in China. *Int J Gynaecol Obstet* 2018;**142**:300–307.

Whitley GS, Cartwright JE. Cellular and molecular regulation of spiral artery remodelling: lessons from the cardiovascular field. *Placenta* 2010;**31**:465–474.

WHO Guidelines. *Guideline on When to Start Antiretroviral Therapy and Pre-exposure Prophylaxis for HIV*. Geneva: World Health Organization, 2015.

Wright JK, Dunk CE, Amsalem H, Maxwell C, Keating S, Lye SJ. HER1 signaling mediates extravillous trophoblast differentiation in humans. *Biol Reprod* 2010;**83**:1036–1045.

Wright JK, Dunk CE, Perkins JE, Winterhager E, Kingdom JC, Lye SJ. EGF modulates trophoblast migration through regulation of Connexin 40. *Placenta* 2006;**27(Suppl A)**:S114–S121.

Zash R, Jacobson DL, Diseko M, Mayondi G, Mmalane M, Essex M, Petlo C, Lockman S, Makhema J, Shapiro RL. Comparative safety of antiretroviral treatment regimens in pregnancy. *JAMA Pediatr* 2017;**171**:e172222.

Zhang Z, Yang X, Zhang L, Duan Z, Jia L, Wang P, Shi Y, Li Y, Gao J. Decreased expression and activation of Stat3 in severe pre-eclampsia. *J Mol Histol* 2015;**46**:205–219.